

Controlling Ice Nucleation during Lyophilization: Process Optimization of Vacuum-Induced Surface Freezing

Andrea Allmendinger ^{1,2,*} , Yuen Li Butt ^{1,2}, Raphael Mietzner ¹ , Felix Schmidt ¹, Joerg Luemkemann ¹ and Carmen Lema Martinez ¹

¹ Pharmaceutical Development & Supplies, Biologics Europe, F. Hoffmann-La Roche, Grenzacherstr. 124, CH-4070 Basel, Switzerland; yuenli_butt@web.de (Y.L.B.); raphael.mietzner@online.de (R.M.); felixschmidt.online@gmail.com (F.S.); joerg.luemkemann@roche.com (J.L.); carmen.lema_martinez@roche.com (C.L.M.)

² Department of Pharmaceutical Technology and Biopharmacy, Institute of Pharmaceutical Sciences, University of Freiburg, Hermann-Herder-Str. 9, D-79104 Freiburg, Germany

* Correspondence: andrea.allmendinger.aa1@roche.com

Received: 14 September 2020; Accepted: 3 October 2020; Published: 8 October 2020



Abstract: Biopharmaceuticals are often lyophilized to improve their storage stability. Controlling ice nucleation during the freezing step of the lyophilization process is desired to increase homogeneity of product properties across a drug product batch and shorten the primary drying time. The present communication summarizes the process optimization of the freezing process when using vacuum-induced surface freezing to control ice nucleation, in particular for amorphous samples. We characterized freeze-dried samples for solid state properties, and compared these to uncontrolled nucleated samples using bovine serum albumin (BSA) as a model protein. Freezing parameters were optimized to obtain complete nucleation, adequate cake resistance during the subsequent lyophilization cycle, and elegant cakes. We highlight the challenges associated with vacuum-induced surface freezing and propose optimized freezing parameters to control ice nucleation, enabling manufacturing of amorphous samples.

Keywords: lyophilization; freeze-drying; controlled ice nucleation; protein formulations; amorphous; sucrose

1. Introduction

Thermolabile drug products, such as biopharmaceuticals, are often stabilized by lyophilization. Water is gently removed from their liquid form to minimize degradation pathways [1–3]. Lyophilization cycles need to be carefully designed in order to obtain safe and high-quality products while minimizing the cycle time and, ultimately, the cost of goods. In particular, the freezing step has been a focal point in recent years [2,4–7].

In conventional freeze-drying cycles, the product is supercooled at a controlled freezing rate to initiate the formation of ice crystals. While ice crystals are forming and growing, formulation components concentrate to the maximal freeze concentrate before complete solidification of the product. In particular, the nucleation temperature defines the size of the ice crystals, which then relates to the pore structure of the final freeze-dried product. A high nucleation temperature is associated with a larger pore size and leads to a higher sublimation rate during primary drying, resulting in a shorter primary drying time [6,8,9]. At the same time, a smaller diffusion rate during secondary drying may lead to higher residual moisture values [10].

The formation of ice crystals is a spontaneous event and, especially in pharmaceutical formulations, it may occur at temperatures far below the equilibrium freezing point of water due to the lack of nucleation seeds. Therefore, nucleation may occur at different temperatures in different containers of the same drug product batch. This implies differences in the pore size distributions for individual samples of the same drug product batch, since the ice crystal size is dependent on the nucleation temperature. For this reason, controlling the ice nucleation temperature is of great interest, as it leads to increased homogeneity of product attributes, such as the residual moisture across a batch [11]. Besides improved inter-vial homogeneity, ice nucleation may be controlled at the highest feasible nucleation temperature, which was demonstrated to shorten primary drying times due to the larger pore size and increased sublimation rate [8].

Several techniques have been described and reviewed in the literature to induce controlled ice nucleation [7,10]. The most common ones include the so-called ice fog technique, where frozen water vapor (ice fog) is created in the lyophilization chamber, which enters the vials and acts as a nucleation seed. The ice fog can be obtained by different measures, as previously described by Rambathla et al. [9], Patel et al. [12], Weija [13], and Geidobler et al. [14]. A second promising technique is described as the depressurization technique in the literature [11,15]. The chamber pressure is increased after equilibration to the desired nucleation temperature before it is rapidly depressurized, which induces ice nucleation. Another technique inducing nucleation by a change in the chamber pressure is referred to as vacuum-induced surface freezing, which is the subject of the present communication.

Vacuum-induced surface freezing to control ice nucleation during the freeze-drying process has been around for years [5,16,17]. A thin layer of ice is formed at the surface of the supercooling solution by the evaporation of water under a vacuum, which propagates nucleation towards the bottom of the vial. The pressure is released immediately to avoid the boiling or blow up of the cake, and the product is subsequently cooled below the glass transition temperature of the solution. In our experience, the application of this technique to crystalline excipients can be straight forward, although we realized that this does not apply for amorphous formulations, such as biopharmaceutical entities. Moreover, severe cake defects, such as boiling of the samples, occurred when using cycle parameters as proposed in the literature. Thus, we aimed for proposing optimized freezing parameters to be used for amorphous protein formulations, which are also applicable in challenging formats such as high-fill or high total solid content formulations. Several improvements have been proposed in the literature for vacuum-induced surface freezing, which we used as a basis and compared to our development. BSA was used as a model protein, and freeze-dried samples were characterized for solid state properties and compared to uncontrolled nucleated samples. The study highlights the challenges associated with vacuum-induced surface freezing and proposes optimized freezing parameters to control ice nucleation.

2. Materials and Methods

2.1. Sample Preparation

Bovine serum albumin (BSA, Sigma Aldrich, Steinheim, Germany) was formulated at a protein concentration of 50 mg/mL in a 20 mM L-histidine/l-histidine-HCL buffer (Ajinomoto, Louvain-la-Neuve, Belgium) at pH 6.0, with the addition of 240 mM sucrose (Ferro Pfanstiehl, Waukegan, Ireland) and 0.02% polysorbate 20 (Croda, Snaith, UK). Formulations were filtered through a Sterivex GV 0.22 µm filter (EMD Millipore, Billerica, MA, USA) and filled under laminar air flow into washed and sterilized 20 mL glass vials (Fiolax clear vials, Schott, Mülheim, Germany) at low and high fill heights of 5.4 mL and 10.6 mL. Vials were stoppered with D1777 lyo stoppers (Daikyo Ltd., Tokyo, Japan).

Samples were lyophilized on a TR01 Lyophilizer (Hof Sonderanlagen, Lohra, Germany) using the corresponding LyoCom III software. The lyophilization cycle was monitored with different process analytical tools. The nucleation event was recorded by a camera through a transparent door using

a GoPro Hero4 (GoPro, Munich, Germany). The chamber pressure during the freezing process was regulated by a capacitive MKS1000 manometer (1–1000 mbar, MKS Instruments Andover, MA, USA) and an MKS10 (0.01–10 mbar) for evacuation before primary drying. The end of primary drying was determined by a Pirani vacuum gauge (0.001–1000 mbar, Edwards, Crawly, UK) when the signal was equal to the MKS10 signal in the chamber (approximately ± 5 μ bar). The product temperature was determined by thermocouples attached to the outside of the vial so as not to induce nucleation.

Cycle optimization was performed with a worst-case configuration of a high total solid content formulation of 10.6 mL and partial load of the lyophilizer. Confirmatory runs, in comparison with an uncontrolled freezing process, were conducted at both fill levels and a full shelf load (middle shelf out of three shelves). Lyophilization parameters are provided for both the uncontrolled and controlled nucleation cycles, with optimized parameters displayed in Table 1. The product temperature was determined by thermocouples placed in the worst-case condition in the middle of the shelf, and also attached to the outside of the vial. Vials were surrounded by one row of empty vials to avoid radiation effects.

Table 1. Freeze-drying parameters for uncontrolled and controlled nucleation runs with optimized parameters.

Uncontrolled Cycle				Controlled Cycle			Purpose			
Cycle Step	Time [hh:mm]	Temp [°C]	Pressure [mbar]	Time [hh:mm]	Temp [°C]	Pressure [mbar]				
Loading	01:00	20	1000	01:00	20	1000	Preparation			
Freezing	-			Cooling of Condenser						
				00:03	20	35	Pressure Ramp ¹			
				00:30	20	35	Degassing			
				00:25	-5	35	Temperature Ramp			
				00:30-03:00 ²	-5	35	Temperature Equilibration			
				00:20	-5	1.35	Induction of Ice Nucleation			
				00:01	-5	100	Aeration to Avoid Boiling			
				Close Isolation Valve						
							01:00	-5	100	Holding Step for Ice Crystal Growth
				03:03	-35	1000	01:40	-35	100	Freezing Ramp
03:00	-35	1000	03:00	-35	100	Complete Freezing				
Primary Drying	00:05	-35	0.13	00:05	-35	0.13	Evacuation ³			
	02:05	-10	0.13	02:05	-10	0.13	Temperature Ramp			
	TBD	-10	0.13	TBD	-10	0.13	Primary Drying Hold Time			
Secondary Drying	02:55	25	0.13	02:55	25	0.13	Temperature Ramp			
	08:00	25	0.13	08:00	25	0.13	Secondary Drying Hold Time			
Stoppering	-	25	700	-	25	700	Stoppering			
Storage	-	5	1000	-	5	1000	Storage			

¹ Use of MKS1000 probe. ² Equilibration time can be shortened depending on fill volume. ³ Use of MKS10 probe. TBD = to be defined, based on Pirani and MKS signals.

2.2. Analytical Characterization

Please refer to Appendix A for details about the following analytical characterization methods used in this study: visual inspection, polydimethylsiloxane embedding, scanning electron microscopy, Karl Fischer titration, specific surface area determination, and reconstitution time determination.

3. Results

The focus of this process development was the lyophilization of amorphous samples, such as formulations containing proteins. Previously proposed process parameters led to product defects such as (a) boiling, (b) deposition of the cake, (c) skin formation, and (d) liquefaction over time, or phase separation of the ice crystals and other solution components as displayed in Figure 1.

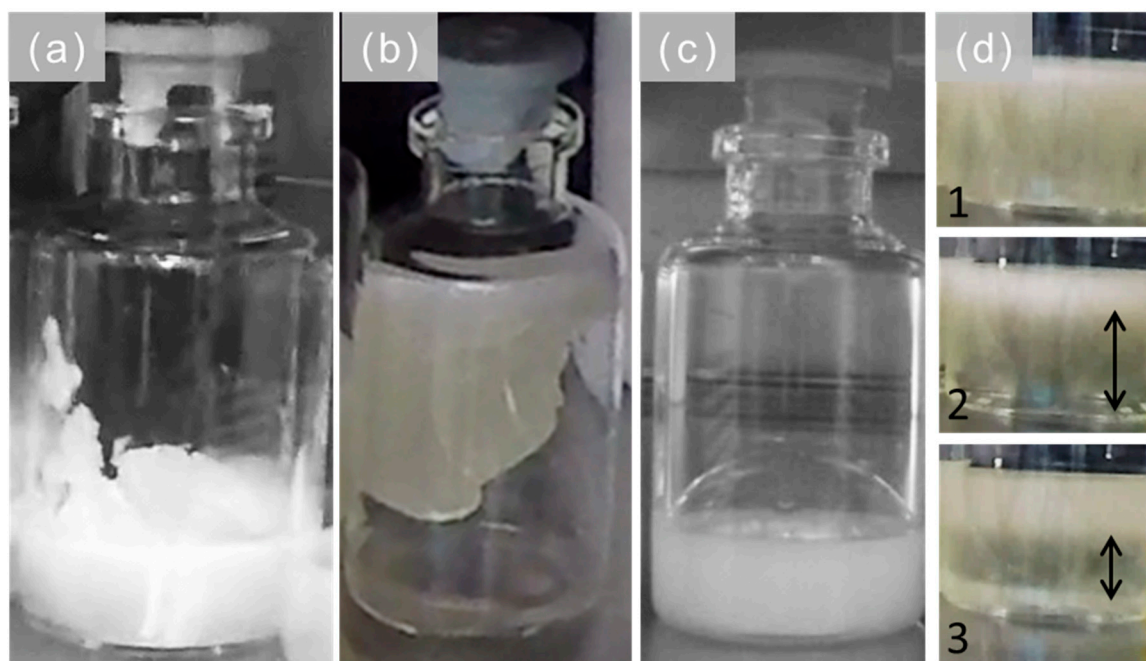


Figure 1. Challenges during cycle optimization using controlled nucleation parameters. (a) Boiling, (b) deposition of the cake, (c) skin formation, and (d) liquefaction over time, as indicated by the black arrows.

Vacuum-induced surface freezing to control ice nucleation was first reported by Kramer et al. (Figure 2a) [16]. They induced ice nucleation at the surface of the solution in the glass vial by reducing the chamber pressure to approximately 1 mbar at a shelf temperature of 10 °C. The vacuum was subsequently released to ambient pressure to inhibit melting of the ice surface while decreasing the shelf temperature to below the onset of the melting point of the ice in the solution. Liu et al. studied a 15% (*w/w*) sulfobutylether 7- β -cyclodextrin solution at a high fill (15/30 mL vial) and showed that the nucleation temperature needs to be optimized and reduced further after nucleation in particular if used without simultaneous pressure release (Figure 2b) [5]. Lowering the shelf temperature after nucleation reduced incomplete nucleation and subsequent spontaneous nucleation and freezing from the bottom of the vial, which resulted in broken cakes after drying [5]. Based on these studies, Oddone et al. proposed to optimize the vacuum control, shorten the vacuum hold step from 5 min [16] to 1 min before pressure release, and combine those parameters with decreasing the shelf temperature after nucleation [5] before further freezing (Figure 2c). Another important modification was closing the valve between the chamber and the condenser once the vacuum set point was reached. The pressure inside the isolated chamber was slightly increased due to the concentrating of water vapor, and therefore the appearance of cake defects was reduced. However, we revealed that the risk of cake blow up was not

completely eliminated, in particular when lyophilizing challenging amorphous formulations at a high total solid content. Hof and Schilder have filed a patent application and proposed a degassing step before inducing nucleation. They suggest parallel ramps in reducing pressure and shelf temperature (Figure 2d) [18]. We combined the degassing step as proposed by Hof and colleagues, the pressure drop and release as proposed by Kramer et al. [16], lowering of the shelf temperature after nucleation [5], and closing the isolation valve between the chamber and condenser after the pressure increase [17]. However, we released the pressure to only 100 mbar to avoid incomplete nucleation, phase separation of ice crystals and other solution components, or liquefaction over time [19].

Figure A1 shows the differences in product temperature, both without pressure release and with pressure release to 100 mbar, indicating melting of the product for the former in particular for the 10.6 mL fill. We further refined the process parameters by optimizing the nucleation temperature to the highest temperature feasible. This means achieving a temperature at which complete nucleation of the solution throughout the vial can be successfully induced and ice crystals can grow during equilibration after nucleation without melting. Depending on the nucleation temperature and the fill volume, the equilibration time of the product to reach the nucleation temperature may need to be adjusted. However, prolongation of the equilibration time may outweigh the reduction in primary drying time, as discussed below. The final process parameters ensured complete nucleation of the samples as studied by visual inspection, with thermocouples attached to the outside of the vials without the described defects. The final process parameters are summarized in Table 1, highlighting the purpose of each process step for the nucleation and freezing process.

We confirmed the outcome of the development runs by lyophilization of the high total solid content BSA formulation at a protein concentration of 50 mg/mL at a low- and high-fill volume. We compared the samples to uncontrolled nucleated vials in terms of product attributes and process performance. Complete nucleation was confirmed for the controlled nucleated vials by visual inspection. Final freeze-dried samples were visually inspected for absence of cake defects. The controlled nucleated samples showed improved cake appearance compared with the uncontrolled nucleated vials without denting (Table 2a), which has been reported previously [10]. However, cake homogeneity did not improve for the controlled nucleated samples, and larger dendritic structures were found at the bottom layer of the vial (Table 2b,c). The specific surface area was smaller, and residual moisture values were higher (Table 2d) for both the low and high fill levels, as expected and reported previously [10]. The secondary drying time was found to be sufficiently long (Figure A2b) without further potential for prolongation to reduce residual moisture contents. Reconstitution times were different between the controlled and uncontrolled samples for the low- and high-fill volumes, with longer reconstitution times for the controlled nucleated vials at a 10.6 mL fill and shorter reconstitution times for the low-fill volume (Table 2d). The longer reconstitution time for the controlled nucleated samples was attributed to the observation of small cake pieces floating on top of the solution before complete dissolution of the product. The primary drying time was shortened for the controlled nucleated samples in the magnitude of a couple of hours, depending on the fill volume. This was confirmed by process monitoring data like the product temperature, determined by thermocouples, and chamber pressure, measured by a Pirani gauge (Figure A2). However, the advantage of a reduced primary drying time might be outweighed by an increased equilibration time for high-fill volume samples, putting the focus of the vacuum-induced surface freezing to control ice nucleation on improved cake appearance and the increased homogeneity of drug product attributes across batches.

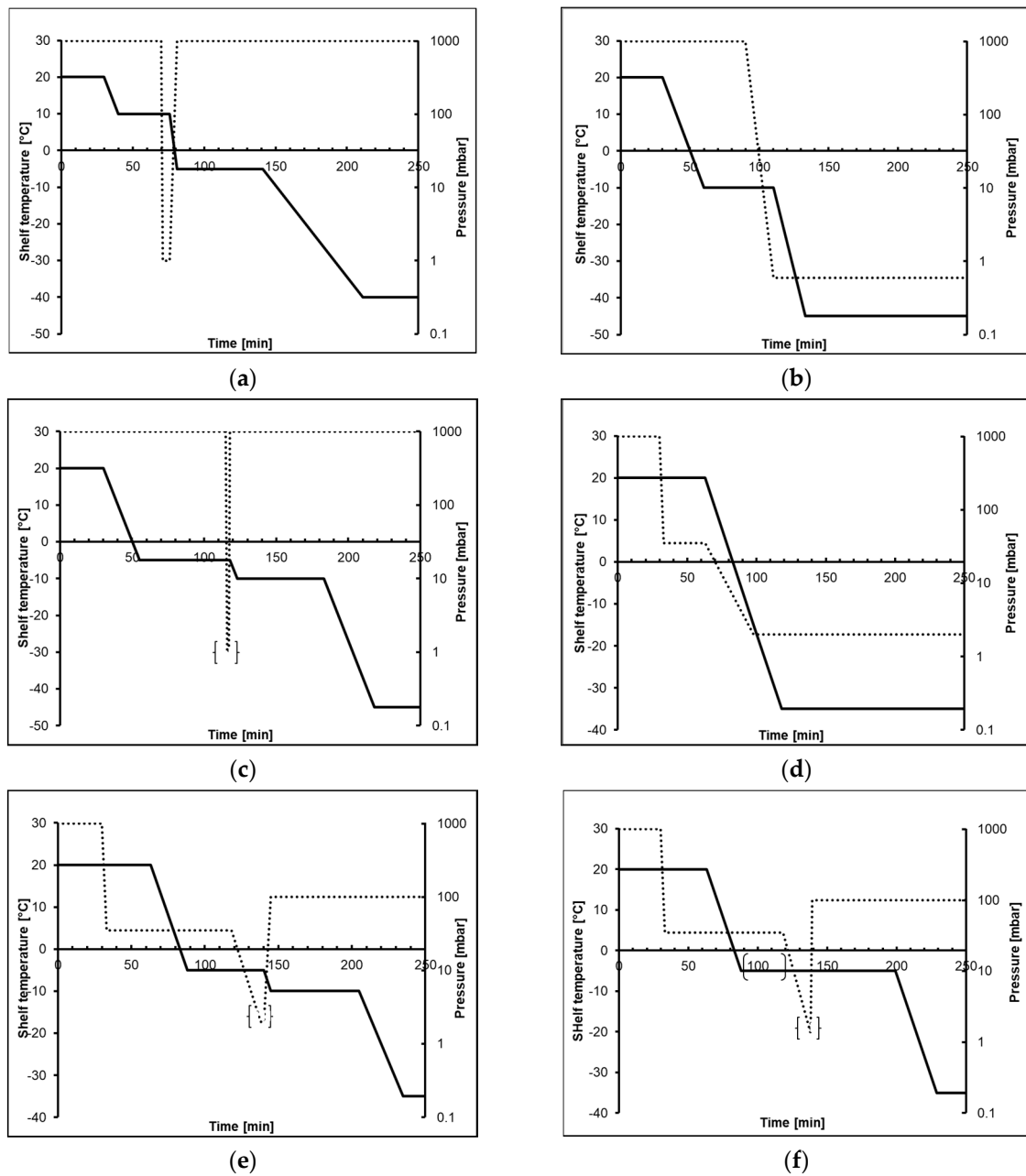
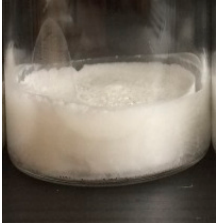

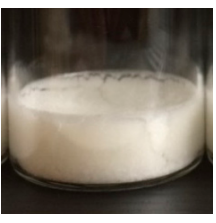
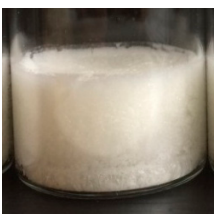
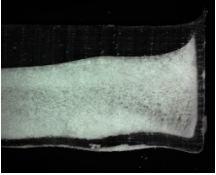
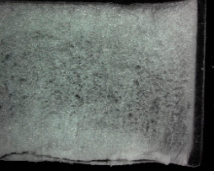

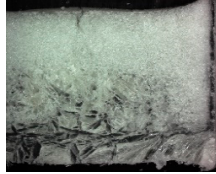
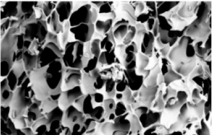
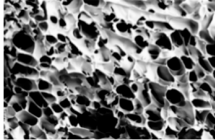
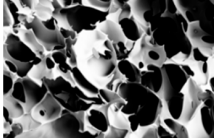
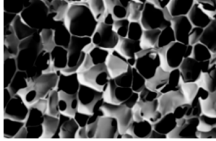
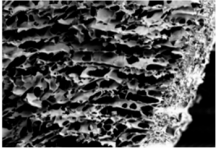
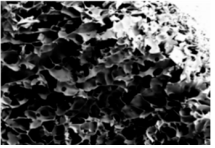
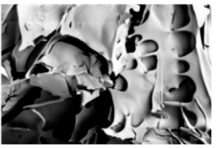
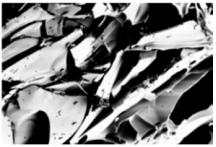
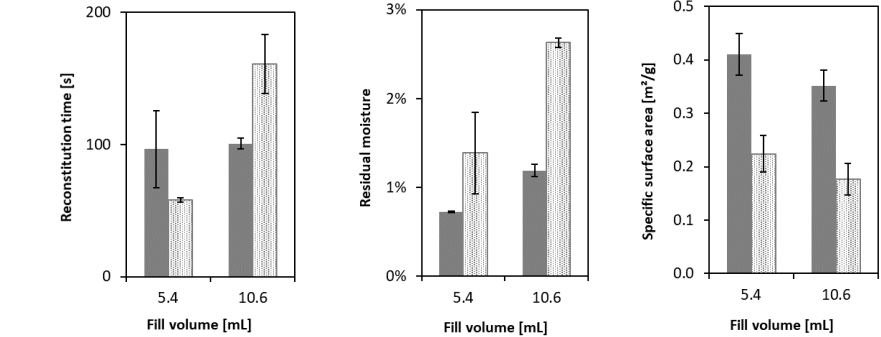


Figure 2. Overview of freezing parameters from the literature, using vacuum-induced surface freezing and proposed optimized parameters from the present study. (a) Kramer et al. [16]; (b) Liu et al. [5]; (c) Oddone et al. [17]; (d) Hof et al. [18]; (e) Allmendinger et al. [19]; and (f) optimized freezing parameters. To compare cycle times, each cycle was adjusted from the literature references to start with equilibration for 30 min at 20 °C (loading temperature). () = equilibration time, dependent on fill volume; { } = closing of the isolation valve.

Table 2. Comparison of product attributes of uncontrolled versus controlled nucleated bovine serum albumin (BSA) formulations at 5.4 and 10.6 mL fill heights in 20 cc vials. (a) Cake appearance by visual inspection, (b) macroscopic cake structure by polydimethylsiloxane (PDMS) embedding, (c) pore structure by SEM, and (d) reconstitution time ($n = 3$), residual moisture ($n = 2$), and specific surface area ($n = 4$). Average values of individual measurements (n) with standard deviation are presented.

		Uncontrolled Nucleation		Controlled Nucleation	
		5.4 mL	10.6 mL	5.4 mL	10.6 mL
(a) Cake Appearance					
(b) Macroscopic Cake Structure					
(c) Pore Structure.	Top				
	Bottom				
(d) Product Attributes					

4. Discussion and Conclusions

The present notes report optimized process parameters for the freezing step during lyophilization when using vacuum-induced surface freezing to control ice nucleation. In particular, successful nucleation is achieved for amorphous formulations, such as proteinaceous formulations, without any cake defects originating from the freezing phase. We propose additional studies to investigate nucleation robustness, especially those dependent on batch size and the size of the lyophilizer. The reported process parameters form the basis for the comparison of vacuum-induced surface freezing to other controlled ice nucleation techniques for both installation and operational considerations,

specifically with regard to product attributes and product stability, published alongside this article in the same issue of this journal.

Author Contributions: Conceptualization and resources, A.A., J.L., and C.L.M.; supervision, project administration, writing—review and editing, A.A. and C.L.M.; methodology, formal analysis, and visualization, Y.L.B., R.M., and F.S.; data curation and writing—original draft preparation, A.A. All authors have read and agreed to the published version of the manuscript.

Funding: This research received no external funding.

Acknowledgments: The authors would like to acknowledge Hof Sonderanlagenbau, and in particular Gerhard Schilder for the initiation and continuous support of this project, Jasmin John, Thomas Steffen, Martin Worgull, Rebecca Rippe, and Denis Luthringer (F. Hoffmann-La Roche, Basel) for their support in the laboratory, Pierre Goldbach (F. Hoffmann-La Roche, Basel), Jacob Luoma, Fred Lim, and Oliver Stauch (Roche Genentech, South San Francisco) for their scientific input, Regine Suess and Heiko Herrklotz from the University of Freiburg, Pharmaceutical Technology and Biopharmacy for supporting this project, and Eva Roedel and Michael Göllner (F. Hoffmann-La Roche, Basel) for their continuous support of the SEM measurements.

Conflicts of Interest: We declare no conflict of interest.

Appendix A. Analytical Panel

Appendix A.1. Visual Inspection

Freeze-dried samples were 100% visually inspected, and cake defects were classified as slight to severe collapse and melt-back, including shrinkage, dents, cracks, and deposition of the lyophilisate in the vial. Representative pictures were taken from each configuration and condition.

Appendix A.2. Polydimethylsiloxane (PDMS) Embedding

To visualize the internal macroscopic cake structure, freeze-dried samples were embedded using PDMS, as previously described by Lam and Patapoff [20]. Sylgard 184 Base and Curing agents (Sylgard® 184 Silicone Elastomer Kit, Dow Corning, MI, USA) were used, and pictures were taken on a Stemi 200 OC microscope (Carl Zeiss AG, Feldbach, Switzerland). Measurements were performed in duplicates.

Appendix A.3. Scanning Electron Microscopy (SEM)

The macro- and micro-structure of the freeze-dried cake was studied by SEM, as previously proposed by Haeuser et al. [21]. Measurements were performed from the top and bottom of a freeze-dried sample.

Appendix A.4. Karl Fischer Titration

Residual moisture was determined by coulometric Karl Fischer titration on a C30 Titrator from Mettler Toledo (Greifensee, Switzerland) and reported as a percent mass of the lyophilized cake. Freeze-dried samples were dissolved in anhydrous methanol 99.8% (Sigma Aldrich, Steinheim, Germany). If not dissolved immediately, samples were gently vortexed or shaken in an ultrasonic bath and left to allow for sedimentation for 15 min before measurement of the supernatant. Measurements were performed in duplicate.

Appendix A.5. Specific Surface Area

The specific surface area of the lyophilized cakes was measured according to the Brunauer–Emmett–Teller (BET) theory on a QuadraSorb Evo™ instrument using QuadraWin™ software (Quantachrome Instruments, Boynton Beach, FL, USA). Samples were prepared by gently crushing ~200 mg of the freeze-dried cake with a spatula into a 9 mm glass bulb. The samples were degassed at 40 °C for at least 3 h using the FloVac® Degaser (Quantachrome) to remove any adsorbed water. The dead volume was subsequently determined with helium. The glass bulb was then cooled with liquid nitrogen during measurement before purging the cell with krypton as an adsorbent. At least five

measurements between 0.05 and 0.3 mbar were conducted, and the specific surface area was reported in m^2/g . Measurements were performed in quadruplicate.

Appendix A.6. Reconstitution Time

Lyophilized samples were dissolved with water for injection (Fresenius, Oberdorf, CH, Switzerland) to the initial fill volume, using a disposable syringe of respective size (BD, Fraga, ES) and a 21G needle. The water was injected through the stopper along the wall of the glass vial to avoid bubble formation. The time was started when all of the water was injected and stopped when the sample was fully dissolved without any visible solid particles. To ensure complete wetting of the cake, the vial was carefully swirled. Measurements were performed in triplicate.

Appendix B

Figure A1 shows the differences in product temperature both without and with pressure release to 100 mbar, indicating melting of the product for the former.

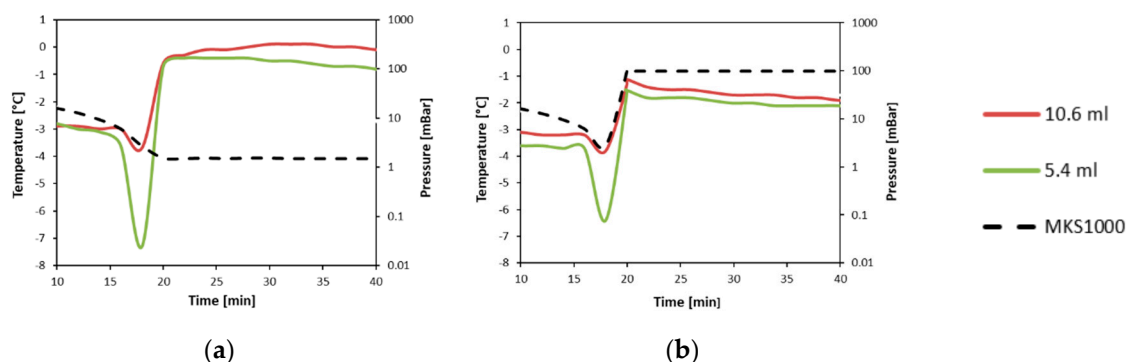


Figure A1. Product temperature for 5.4 mL and 10.6 mL fill volumes during the nucleation event (a) without and (b) with pressure increase to 100 mbar. Product temperature was measured with a thermocouple at the outside of the vial. The pressure was monitored by an MKS10 pressure probe.

Figure A2 shows process monitoring data, such as the product temperature determined by the thermocouples and chamber pressure, measured by a Pirani and MKS10 gauge, indicating shortening of the primary drying time for controlled nucleated samples compared with uncontrolled nucleated samples (Figure A2a).

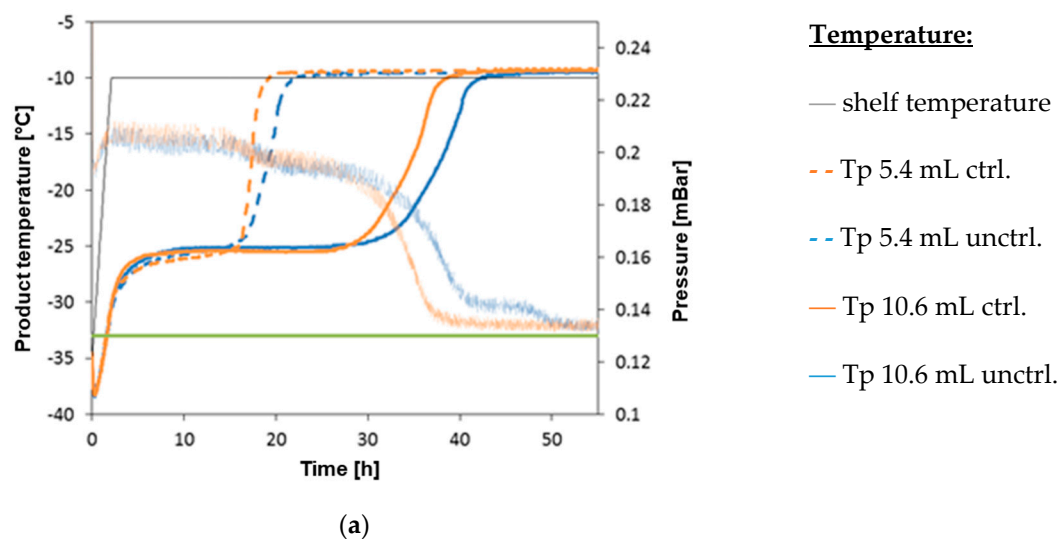


Figure A2. Cont.

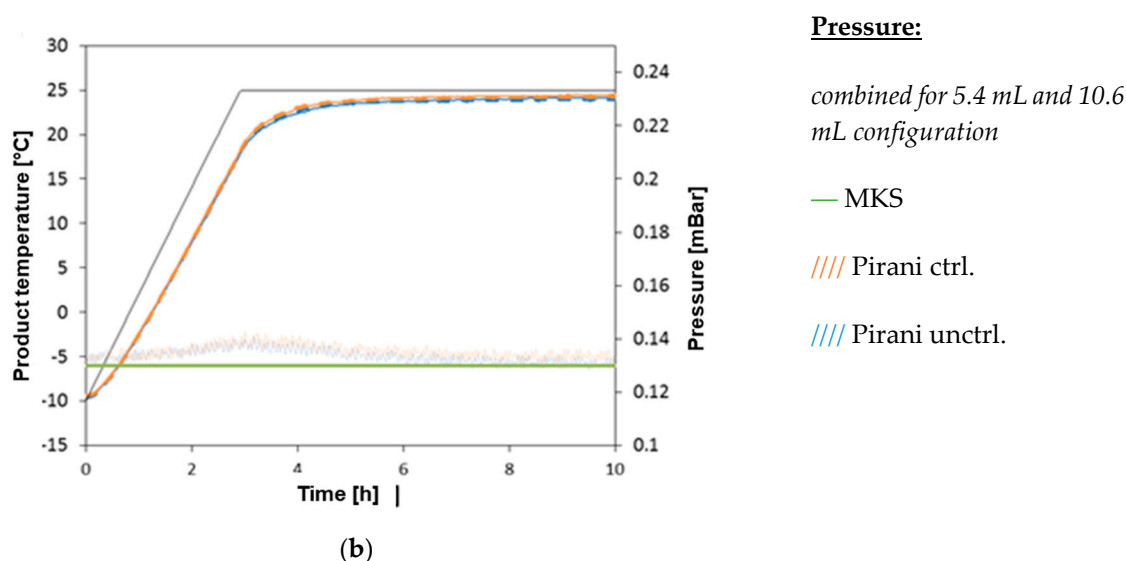


Figure A2. Process monitoring data for 5.4 mL and 10.6 mL fill volumes for controlled (ctrl.) and uncontrolled (unctrl.) nucleated samples. The product temperature (T_p) was determined by thermocouples that were attached to the outside of the vial. The chamber pressure was measured by a Pirani gauge and an MKS10 probe. (a) Primary drying. (b) Secondary drying.

References

- Manning, M.C.; Chou, D.K.; Murphy, B.M.; Payne, R.W.; Katayama, D.S. Stability of protein pharmaceuticals: An update. *Pharm. Res.* **2010**, *27*, 544–575. [[CrossRef](#)] [[PubMed](#)]
- Bhatnagar, B.; Tchessalov, S. Advances in Freeze Drying of Biologics and Future Challenges and Opportunities. In *Drying Technologies for Biotechnology and Pharmaceutical Applications*, 1st ed.; Satoshi Ohtake, S., Izutsu, K.I., Lechuga-Ballesteros, D., Eds.; Wiley-VCH: Weinheim, Germany, 2020; pp. 137–177.
- Kasper, J.C.; Winter, G.; Friess, W. Recent advances and further challenges in lyophilization. *Eur. J. Pharm. Biopharm.* **2013**, *85*, 162–169. [[CrossRef](#)] [[PubMed](#)]
- Kasper, J.C.; Friess, W. The freezing step in lyophilization: Physico-chemical fundamentals, freezing methods and consequences on process performance and quality attributes of biopharmaceuticals. *Eur. J. Pharm. Biopharm.* **2011**, *78*, 248–263. [[CrossRef](#)] [[PubMed](#)]
- Liu, J.; Viverette, T.; Virgin, M.; Anderson, M.; Paresh, D. A study of the impact of freezing on the lyophilization of a concentrated formulation with a high fill depth. *Pharm. Dev. Technol.* **2005**, *10*, 261–272. [[CrossRef](#)] [[PubMed](#)]
- Searles, J.A.; Carpenter, J.F.; Randolph, T.W. The ice nucleation temperature determines the primary drying rate of lyophilization for samples frozen on a temperature-controlled shelf. *J. Pharm. Sci.* **2001**, *90*, 860–871. [[CrossRef](#)] [[PubMed](#)]
- Geidobler, R.; Winter, G. Controlled ice nucleation in the field of freeze-drying: Fundamentals and technology review. *Eur. J. Pharm. Biopharm.* **2013**, *85*, 214–222. [[CrossRef](#)] [[PubMed](#)]
- Konstantinidis, A.K.; Kuu, W.; Otten, L.; Nail, S.L.; Sever, R.R. Controlled nucleation in freeze-drying: Effects on pore size in the dried product layer, mass transfer resistance, and primary drying rate. *J. Pharm. Sci.* **2011**, *100*, 3453–3470. [[CrossRef](#)] [[PubMed](#)]
- Rambhatla, S.; Ramot, R.; Bhugra, C.; Pikal, M.J. Heat and mass transfer scale-up issues during freeze drying: II. Control and characterization of the degree of supercooling. *AAPS PharmSciTech* **2004**, *5*, 54–62. [[CrossRef](#)] [[PubMed](#)]
- Awotwe-Otoo, D.; Agarabi, C.; Read, E.K.; Lute, S.; Brorson, K.A.; Khan, M.A.; Shah, R.B. Impact of controlled ice nucleation on process performance and quality attributes of a lyophilized monoclonal antibody. *Int. J. Pharm.* **2013**, *450*, 70–78. [[CrossRef](#)] [[PubMed](#)]

11. Luoma, J.; Magill, G.; Kumar, L.; Yusoff, Z. Controlled Ice Nucleation Using ControLyo® Pressurization-Depressurization Method. In *Lyophilization of Pharmaceuticals and Biologicals—New Technologies and Approaches*, 1st ed.; Ward, K., Matejtschuk, P., Eds.; Humana Press: New York, NY, USA, 2019; pp. 57–77.
12. Patel, S.M.; Bhugra, C.; Pikal, M.J. Reduced pressure ice fog technique for controlled ice nucleation during freeze-drying. *AAPS PharmSciTech* **2009**, *10*, 1406–1411. [[CrossRef](#)] [[PubMed](#)]
13. Ling, W. Controlled Nucleation during Freezing Step of Freeze Drying Cycle Using Pressure Differential Ice Fog Distribution. U.S. Patent 8839528B2, 29 April 2011.
14. Geidobler, R.; Mannschedel, S.; Winter, G. A new approach to achieve controlled ice nucleation of supercooled solutions during the freezing step in freeze-drying. *J. Pharm. Sci.* **2012**, *101*, 4409–4413. [[CrossRef](#)] [[PubMed](#)]
15. Rampersad, B.S.; Sever, R.R.; Hunek, B.; Gasteyer, T.H. Freeze-Dryer and Method of Controlling the Same. U.S. Patent 8240065B2, 14 August 2012.
16. Kramer, M.; Sennhenn, B.; Lee, G. Freeze-drying using vacuum-induced surface freezing. *J. Pharm. Sci.* **2002**, *91*, 433–443. [[CrossRef](#)] [[PubMed](#)]
17. Oddone, I.; Van Bockstal, P.J.; De Beer, T.; Pisano, R. Impact of vacuum-induced surface freezing on inter- and intra-vial heterogeneity. *Eur. J. Pharm. Biopharm.* **2016**, *103*, 167–178. [[CrossRef](#)] [[PubMed](#)]
18. Hof, H.G.; Schilder, G. Verfahren zur Gefriertrocknung eines mit einem Lösungsmittel versehenen, feuchten Produktes. EP2728287A2, 24 August 2013.
19. Allmendinger, A.; Schilder, G.; Mietzner, R.; Butt, Y.L.; Luemkemann, J.; Lema Martinez, C.; Controlled Nucleation during Freeze Drying Using Vacuum-Induced Surface Freezing. Invention disclosure rd633018. 2017. Available online: <http://www.researchdisclosure.com> (accessed on 24 July 2020).
20. Lam, P.; Patapoff, T.W. An improved method for visualizing the morphology of lyophilized product cakes. *PDA J. Pharm. Sci. Technol.* **2011**, *65*, 425–430. [[CrossRef](#)] [[PubMed](#)]
21. Haeuser, C.; Goldbach, P.; Huwyler, J.; Friess, W.; Allmendinger, A. Be Aggressive! Amorphous Excipients Enabling Single-Step Freeze-Drying of Monoclonal Antibody Formulations. *Pharmaceutics* **2019**, *11*, 616. [[CrossRef](#)] [[PubMed](#)]



© 2020 by the authors. Licensee MDPI, Basel, Switzerland. This article is an open access article distributed under the terms and conditions of the Creative Commons Attribution (CC BY) license (<http://creativecommons.org/licenses/by/4.0/>).